https://doi.org/10.5194/acp-2021-834
Preprint. Discussion started: 6 October 2021

Atmospheric Chemistry and Physics Discussions

Insights into the abnormal increase of ozone during COVID-19 in a typical urban city of China

Kun Zhang [a, b#], Zhiqiang Liu [a, c#], Xiaojuan Zhang [a, c], Qing Li [a, b], Andrew Jensen [d, e], Wen Tan [f], Ling Huang [a, b], Yangjun Wang [a, b], Joost de Gouw [d, e], Li Li [a, b*]

[a] School of Environmental and Chemical Engineering, Shanghai University, Shanghai, 200444, China

[b] Key Laboratory of Organic Compound Pollution Control Engineering, Shanghai University, Shanghai, 200444, China

[c] Changzhou Institute of Environmental Science, Changzhou, Jiangsu, 213022, China

[d] Cooperative Institute for Research in Environmental Sciences, University of Colorado, Boulder, Colorado, 80309, USA

[e] Department of Chemistry, University of Colorado, Boulder, Colorado, 80309, USA

[f] Tofwerk AG, Thun, Switzerland

[#] These authors contribute equally to this work.

Correspondence: Li Li (lily@shu.edu.cn)

Abstract

The outbreak of COVID-19 promoted strict restrictions to human activities in China, which led to dramatic decrease in most air pollutant concentrations (e.g., $PM_{2.5}$, PM_{10}, NO_x, SO_2, and CO). However, abnormal increase of ozone (O_3) concentrations was found during the lockdown period in most urban areas of China. In this study, we conducted a field measurement targeting ozone and its key precursors by utilizing a novel proton transfer reaction time-of-flight mass spectrometer (PTR-TOF-MS) in Changzhou, which is representative for the Yangtze River Delta (YRD) city cluster of China. We further applied the integrated methodology including machine learning, observation-based model (OBM), and sensitivity analysis to get insights into the reasons causing the abnormal increase of ozone. Major

https://doi.org/10.5194/acp-2021-834
Preprint. Discussion started: 6 October 2021


Atmospheric Chemistry and Physics Discussions

findings include: (1) By deweathered calculation, we found changes in precursor emissions contributed 5.1 ppbv to the observed O_3 during the Full-lockdown period, while meteorological conditions only contributed 0.5 ppbv to the O_3 changes. (2) By using an OBM model, we found that although significant reduction of O_3 precursors was observed during Full-lockdown period, the photochemical formation of O_3 was stronger than that during the Pre-lockdown period. (3) The NO_x/VOCs ratio dropped dramatically from 1.84 during Pre-lockdown to 0.79 in Full-lockdown period, which switched O_3 formation from VOCs-limited regime to the conjunction of NO_x- and VOC-limited regime. Additionally, the decrease in NO_x/VOCs ratio during Full-lockdown period was supposed to increase the MeanO_3 by 2.4 ppbv. Results of this study investigate insights into the relationship between O_3 and its precursors in urban area, demonstrating reasons causing the abnormal increase of O_3 in most urban areas of China during the COVID-19 lock-down period. This study also underlines the necessity of controlling anthropogenic OVOCs, alkenes, and aromatics in the sustained campaign of reducing O_3 pollution in China.

Keywords: Ozone; VOCs; PTR-TOF-MS; COVID-19

1. Introduction

At the end of 2019, a tragic coronavirus (COVID-19) occurred, which has caused over 184 million global infection and over 3.99 million deaths as of this writing (5 Jun 2021). To protect people's health, China adopted strict measures to control the spread of this pandemic. Thirty provinces, autonomous regions and municipalities have launched Full-lockdown response (also known as Level I response, roughly from 24 Jan to 25 Feb 2020) as early as 24 Jan 2020 (Shen et al., 2021; Li et al., 2020; Huang et al., 2020). With the effective control of COVID-19 in China, the emergency response level in most provinces (except Hubei province, the hardest-hit region) gradually downgraded to Partial-lockdown (Level II and Level III response, roughly after 25 Jan 2020) (Li et al., 2020), and work resumption started. During Full-lockdown period, all the social events that may cause crowds (excluding transportation and industries that maintained the basic operation of society) were severely restricted. Affected by the pandemic, many factories were shut down, and the on-road traffic volume and

https://doi.org/10.5194/acp-2021-834
Preprint. Discussion started: 6 October 2021


Atmospheric Chemistry and Physics Discussions

53 construction activities have been reduced significantly (Zheng et al., 2020). During Full-lockdown
54 period, dramatic decrease of air pollutants (e.g., $PM_{2.5}$, NO_2, BC) were found in China, especially in
55 urban areas (Fan et al., 2021; Gao et al., 2021; Li et al., 2020; Xu et al., 2020). Surprisingly, marginal
56 increases of O_3 were observed during the lockdown period in YRD region, and this seems to be
57 contradictory to the decrease of most air pollutants (Li et al., 2020). However, as suggested by previous
58 studies, the formation of O_3 is significantly influenced by NO_x/VOCs ratio and meteorological
59 conditions (temperature and relative humidity) (Zhang et al., 2020a; Zhang et al., 2020b). Therefore, it
60 is essential to investigate the changes of meteorological and emissions conditions to figure out reasons
61 causing the abnormal increase of O_3 during this pandemic.

62 Previous studies on the O_3 pollution in the YRD region have often focused on the more populated
63 metropolitan areas, such as Shanghai and Nanjing, which are considerably far away from the industrial
64 zones that are essentially responsible for the sources of O_3 precursors (Li et al., 2019; Zhang et al.,
65 2020b). Changzhou, located in the center of the Yangtze River Delta (YRD) region, is a typical city with
66 fast urbanization, heavy industrial structure, huge energy consumption, increasing vehicle stocks and
67 frequent air pollution. Therefore, it provides a more representative environment to fully elucidate the
68 mechanism underlying the O_3 pollution in the YRD region (Shi et al., 2020). In a companion paper
69 (Jensen et al., 2021), we also demonstrated that Changzhou is representative for the region by analyzing
70 both surface observations and satellite data. According to previous studies, the anthropogenic VOCs
71 emission in Changzhou was around 9~12.6×10^4 tons/year, among which industries was the dominant
72 source, accounting for 27~47% of the total VOC emissions (Cheng et al., 2016; Fu et al., 2013). It is
73 notable that industrial sources together contributed over 80% of anthropogenic VOC emissions (Sun et
74 al., 2019). Apart from industrial sources, vehicle exhaust accounted for 9%~14% of total VOC
75 emissions (Sun et al., 2019). However, rare observation regarding VOCs characteristics during COVID-
76 19 in Changzhou has been conducted.

77 Highly time-resolved measurements of VOCs are generally much sparser and could not be easily
78 expanded during the lockdowns. This limits our understanding of how VOCs changed and how the
79 formation of ozone was affected. Here, we used a novel proton transfer reaction time-of-flight mass

https://doi.org/10.5194/acp-2021-834
Preprint. Discussion started: 6 October 2021

Atmospheric Chemistry and Physics Discussions

spectrometer (PTR-TOF-MS, Tofwerk, Model Vocus Elf, CHE) to conduct online observation of VOCs in Changzhou. The characteristics of VOCs and the variations of general air pollutants in each emergency response period were analyzed. Additionally, ozone formation during each period was investigated by an OBM model. Although terrifying impact has been caused by the COVID-19, it provided a rare experiment to analyze the variations of VOCs and NO_x due to changes of anthropogenic activities in a typical city of China. Furthermore, results of this study offer theoretical support for formulating refined ozone management policy in China.

2. Methodology

2.1 Field measurement

The field campaign was conducted from 8 Jan to 31 Mar 2020 at a sampling site located on the rooftop of a building at Changzhou Environmental Monitoring Center (CEMC, 31.76° N, 119.96° E), which was approximately 15 m above ground level. As a typical urban monitoring station, this site is in the center of Changzhou city, surrounded by residential and commercial area, which is also adjacent to the main transportation junction in Changzhou (Figure 1). According to local epidemic prevention policies, we roughly classified the measurement periods into three stages: Pre-lockdown (8th January to 23rd January 2020), Full-lockdown (25th January to 24th February 2020), Partial-lockdown (25th February to 28th March 2020) as defined in a study of the Yangtze River Delta (Li Li et al., 2020).

https://doi.org/10.5194/acp-2021-834
Preprint. Discussion started: 6 October 2021

Atmospheric Chemistry and Physics Discussions

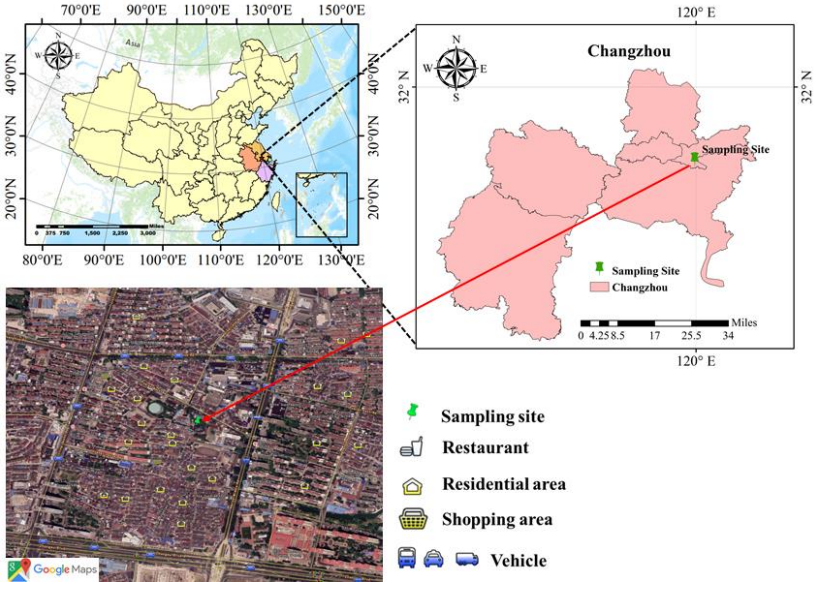

Figure 1. Location of the sampling site in Changzhou (© Google Maps).

From Jan 8 to Mar 27, 2020, the concentrations of traditional air pollutants ($PM_{2.5}$, PM_{10}, NO_x, SO_2, CO, O_3) as well as meteorological parameters were monitored by a series of analyzers (Table 1). In particular, 87 VOCs species were quantified, 59 of which were identified, by a PTR-TOF-MS with time resolution of 1 min. Detailed measurement techniques and quality assurance and control has been documented in detail in our companion paper (Jensen et al., 2021). Here, we just briefly introduce the measurement. The air samples were directly inhaled into the 3 m-long tube connected to the instrument. A priming pump, with flow rate of 4 L/min, was used to reduce the retention time of the gas sample in the tube. To avoid blocking of inlet tube caused by particles, a particulate filter was assembled at the front of the inlet tube. The pressure of the ion source was set as 2 mbar and the temperature of the reaction chamber was set to 90 °C during the observation. The PTR-TOF-MS can detect most unsaturated hydrocarbons and VOCs with functional groups but cannot detect species with proton affinities lower than that of water, namely alkanes and small alkenes. Eighteen standard gases (including acetonitrile, acetaldehyde, acrolein, acetone, isoprene, butanone, 2-butanone, benzene, 2-pentanone, ethyl acetate, toluene, methyl isobutyl ketone, styrene, xylene, trimethylbenzene, naphthalene, a-pinene, and 1,3-dichlorobenzene) with concentrations of 1 ppmv were used for the calibration of the PTR-TOF-

https://doi.org/10.5194/acp-2021-834
Preprint. Discussion started: 6 October 2021


Atmospheric Chemistry and Physics Discussions

MS. In addition, a built-in calibration system was used to control the zero and standard gases.

Table 1 Measurements performed during the field campaign.

Species/Parameter	Experimental Technique
T, RH, WS, WD and P	2000WX, Airmax, USA
O_3	400E, API, USA
NO_x (NO and NO_2)	T200, API, USA
SO_2	T100, API, USA
CO	T300, API, USA
$PM_{2.5}$	5030, Thermo Fisher, USA
PM_{10}	5030, Thermo Fisher, USA
VOCs	Vocus Elf, Tofwerk, CHE

2.2 Observation-based model

An OBM model coupled with MCM v3.3.1 was utilized to investigate the atmospheric oxidation capability and the radical chemistry. Detailed information about the chemistry mechanism is available on MCM website (http://mcm.leeds.ac.uk/MCM/, last access 8 Jul 2021). More than 5800 chemical species and 17000 reactions are included in this mechanism. The photolysis frequencies (J values) were calculated based on the trigonometric parameterization provided by MCM (Wolfe et al., 2016). Dilution mixing within the boundary layer is considered. However, as a 0-zero model, vertical or horizonal transport of airmasses are not involved. The observed meteorological parameters (T, RH, P), trace gases (NO, NO_2, CO, SO_2, and VOCs) were used to constrain the model. Before each simulation, the model was run 3 days as spin-up to reach a stable state. According to the definition of atmospheric oxidation capability (AOC), AOC is quantified by Eq (1) (Zhu et al., 2020).

$$AOC = \sum_i k_{Y_i}[Y_i][X] \quad (1)$$

where Y_i are the primary pollutants (e.g., VOCs, CH_4, and CO); X are atmospheric oxidants (OH, O_3, NO_3); k_{Yi} are the bimolecular rate constants for the reactions of Y_i and X. A high value of AOC indicates fast scavenge of primary air pollutants. Additionally, OH reactivity (k_{OH}), defined as the reaction rate

https://doi.org/10.5194/acp-2021-834
Preprint. Discussion started: 6 October 2021


Atmospheric Chemistry and Physics Discussions

coefficients multiplied by the concentrations of the reactants with OH, is also widely used as an indicator of AOC. The value of k_{OH} depends on both the abundances and compositions of primary pollutants and can be calculated by Eq (2).

$$k_{OH} = \sum_i k_{(OH+X_i)} \times [X_i] \quad (2)$$

where $k_{(OH+Xi)}$ are the reaction rate coefficients of reaction OH+X_i; X_i are the concentrations of pollutants (VOC, NO_2, CO, OVOC etc.) (Zhu et al., 2020).

2.3 Trend Analysis

Mann-Kendall (MK) trend test is a widely used non-parametric test method (Pathakoti et al., 2021; Zhang et al., 2013), which is recommended by the World Meteorological Organization. It is applicable to all distributions (that is, the data does not need to meet the assumption of normal distribution), but the data should have no serial correlation. If the data has serial correlation, it will have an impact on the significance level (p value). In this study, the MK trend analysis was performed for individual VOC concentrations during Pre-lockdown and Full-lockdown period. Detailed description of this method could be found in the study of Pathakoti et al. (2021) and Alhathloul et al. (2021). A positive z value from the MK test indicates increasing trend of the target compound. On the contrary, a negative z value suggests the target compound was decreasing.

Sen's slope, a non-parametric test proposed by Sen (1968), is also used in this study to assess the rate of change in individual VOC concentrations. Sen's slope (Q) is mathematically represented by the following equations.

$$Q = median(SS_{ij}) \quad (3)$$

$$SS_{ij} = \frac{x_j - x_i}{j - i}, 1 \le i \le j \le n \quad (4)$$

where x_j and x_i are concentrations of VOC specie x at time j and i ($1 \le i \le j \le n$), respectively. SS_{ij} is the linear slope between time i and j, and Q is the median of SS_{ij}. Positive and negative Q values indicating increasing or decreasing trend of VOC specie x, respectively.

2.4 Deweathered model

https://doi.org/10.5194/acp-2021-834
Preprint. Discussion started: 6 October 2021


Atmospheric Chemistry and Physics Discussions

153 The observed concentrations of O_3 could be influenced by meteorological conditions,
154 emissions/chemistry. To quantitatively assess the contribution of meteorological conditions and
155 emissions/chemistry, the deweathered O_3 concentrations was calculated based on the random forest (RF)
156 approach. The number of trees in the RF model was set as 300, the minimal node size was five, and the
157 number of samples was 300. Hourly data of Unix date (number of seconds since 1970-01-01), Julian
158 day, weekday, hour of day, wind speed (WS), wind direction (WD), temperature (T), relative humidity
159 (RH), and pressure (P) were used for the deweathered calculation of O_3. More details of this model
160 could be found in the study of Grange and David (2019).

161 # 3. Results and discussion

162 ## 3.1 Overview of the field campaign

163 Figure 2 shows the meteorological conditions during the observation. During the whole experiment,
164 the prevailing WD was southeast. The average T and RH was 9.9 ± 5.1°C and 58.9 ± 17.1%, respectively.
165 Compared to Pre-lockdown period, the concentrations of $PM_{2.5}$, PM_{10}, SO_2, NO, NO_2, TVOC and CO
166 during Full-lockdown period decreased by 48%, 42%, 11%, 65%, 58%, 33% and 39%, respectively. It
167 is interesting to note that the decreasing ratio of VOC : NO_x is around 1:2. Meanwhile, the average O_3
168 concentrations in Full-lockdown period was 67% higher than that during Pre-lockdown period. To
169 estimate whether the increase of O_3 during Full-lockdown period is abnormal, we summarized the
170 meteorological conditions and O_3 concentrations during the same period in 2020 and 2019 (Table 2 and
171 Figure 3). It should be noted that, considering the influence of Chinese New Year, the corresponding
172 period in 2019 was decided according to lunar calendar. Compared to Full-lockdown period in 2019,
173 the mean O_3 concentration in 2020 was 5.5 ppbv higher (Figure 2). The T and RH in Full-lockdown
174 period in 2020 was ~1.6 °C higher and 6.1% lower than that in the same period in 2019, while the P and
175 WS were comparable during the same period in 2020 and 2019. The relatively higher T and lower RH
176 condition was supposed to be in favor of O_3 formation during the Full-lockdown period in 2020.
177 Additionally, we compared the hours of adverse weather conditions (with RH >70% and WS <1m/s)
178 and found that the meteorological condition during Full-lockdown period in 2020 restrained the dilution

https://doi.org/10.5194/acp-2021-834
Preprint. Discussion started: 6 October 2021

Atmospheric Chemistry and Physics Discussions

of air pollutants (Table 2). Therefore, the meteorological conditions during Full-lockdown period in 2020 seemed to favor O_3 formation. However, changes in O_3 concentrations could be a result of the joint effect of meteorological conditions and emissions/chemistry, the following sections would discuss the influences respectively.

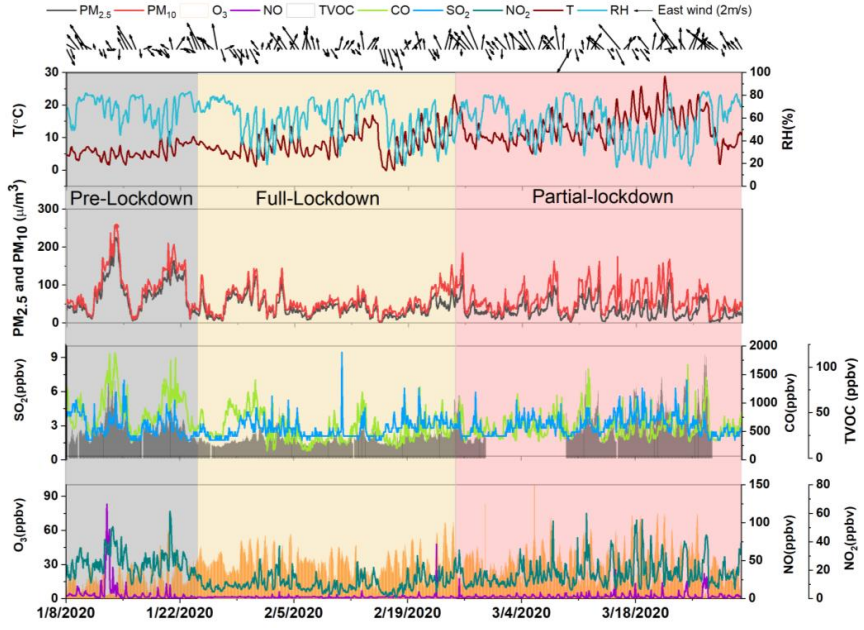

Figure 2 Time series of meteorological parameters and air pollutants during the whole observation.

Table 2 Comparison of average meteorological conditions during Pre-lockdown, Full-lockdown, and Partial-lockdown period in 2020 and the same period in 2019.

Periods	Date	P (hPa)	RH (%)	T (℃)	Precipitation (mm)	WS (m/s)	Adverse weather conditions*	
							Number of hours (h)	Proportion (%)
Pre-lockdown	(2020.1.8-1.24)	1025.4	84.9	4.8	0.13	1.8	54	17.5%
Same period in 2019	(2019.1.19-2.4)	1025.6	72.7	5.2	0.05	1.9	70	18.5%
Full-lockdown	(2020.1.25-2.24)	1025.6	73.0	7.3	0.09	2.1	103	15.6%
Same period in 2019	(2019.2.5-3.7)	1024.1	79.1	5.7	0.15	2.1	82	13.7%
Partial-lockdown	(2020.2.25-3.31)	1018.9	69.5	12.1	0.11	2.4	106	12.3%
Same period in 2019	(2019.3.8-4.12)	1017.6	64.	13.8	0.02	2.	72	8.3%

* The non-rainfall periods with RH less than 70% and WS below 1m/s were defined as adverse weather condition.

3.2 Mechanism affecting the abnormal O_3 increase

https://doi.org/10.5194/acp-2021-834
Preprint. Discussion started: 6 October 2021

Atmospheric Chemistry and Physics Discussions

3.2.1 Meteorological perspective

Deweathered O_3 concentrations were calculated based on the model described in Section 2.4. The random forest model grown for O_3 at the sampling site had R^2 values of 0.84, therefore, the model shows good performance for O_3 predictions. The difference between observed ($O_{3,Obs}$) and weather-normalized O_3 ($O_{3,Normal}$) can be regarded as the meteorological influence ($O_{3,Met}$). In addition, the difference between $O_{3,Obs}$ concentrations in different years could be considered as the influence of emissions ($O_{3,Emi}$). Figure 3 exhibited the average $O_{3,Obs}$, $O_{3,Normal}$, $O_{3,Met}$ during the same periods in 2019 and 2020, respectively. The mean $O_{3,Normal}$ during Pre-lockdown and Partial-lockdown periods in 2019 and 2020 were close, suggesting the similar emission condition during these periods in 2019 and 2020. During Full-lockdown period in 2020, $O_{3,Met}$ contributed +0.5 ppbv to $O_{3,Obs}$, which is consistent with the rough summary of meteorological conditions in Table 2, confirming that the weather conditions during the Full-lockdown period in 2020 favored O_3 formation. However, the average $O_{3,Normal}$ during Full-lockdown period in 2020 was 5.1 ppbv higher than that in 2019, indicating that improper decline of precursor emissions was possibly the key reason for the abnormal increase of O_3 during Full-lockdown period in 2020.

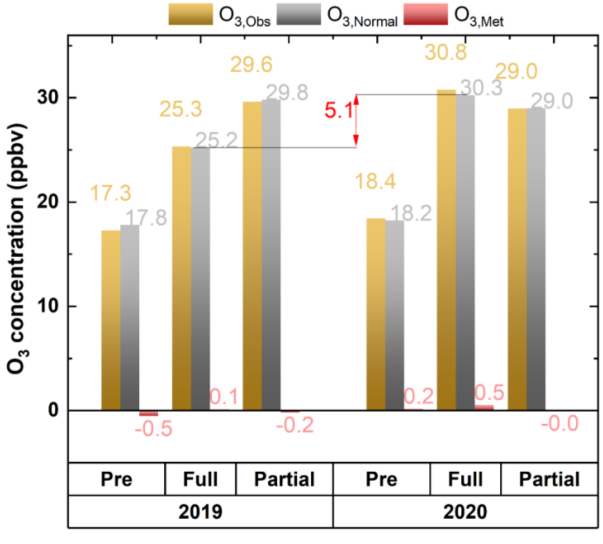

Figure 3. Comparison of observed (Obs), weather-normalized (Normal), and meteorological-factors-infected (Met) O_3 concentrations during the same period in 2019 and 2020.

https://doi.org/10.5194/acp-2021-834
Preprint. Discussion started: 6 October 2021

Atmospheric Chemistry and Physics Discussions

3.2.2 Ambient VOCs

As mentioned above, the changes in O_3 precursor emissions strongly affected the $O_{3,Obs}$, and the changes in VOCs and NO_x emissions would eventually be reflected by the observed concentrations of individual VOCs and NO_x. Therefore, the concentrations of each VOC group in different periods were summarized (Figure 4). OVOCs dominated the total VOCs (TVOC) concentrations during the whole observation, with a daily average concentration of 21.44 ± 10.27 ppbv. During Full-lockdown period, the TVOC dropped to 22.19 ±7.9 ppbv, which was mainly affected by the decrease in industrial activities and traffic volume. The most obvious drop was found in aromatics (~54%), followed by OVOCs (~27%), alkenes (~26%), nitrogen hydrocarbon (~25%), and other VOCs (~21%). Additionally, the discrepancy of daytime and nighttime VOCs concentrations during different periods were compared (Figure 4 (A)). Interestingly, the concentration of each VOCs group exhibited higher values during nighttime, which was caused by the low atmospheric oxidation condition and the low atmospheric boundary layer height (Maji et al., 2020; Valach et al., 2015).

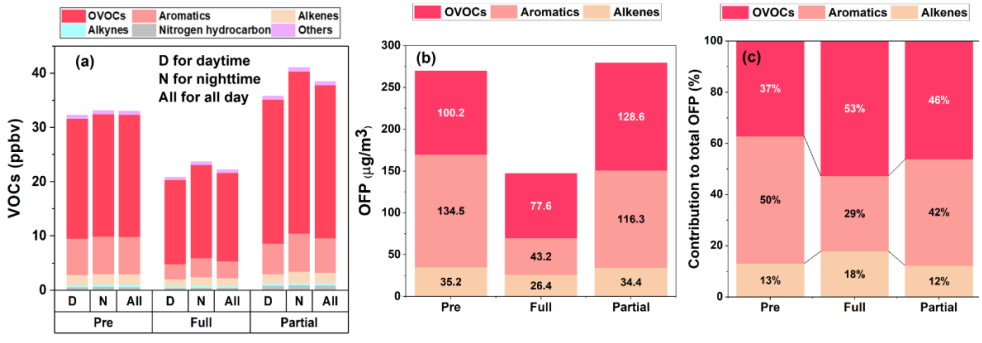

Figure 4. Comparison of daytime and nighttime VOCs concentrations (A), average OFP (B), and contribution to total OFP (C) during different periods.

Furthermore, the average concentrations of individual VOCs during different periods were summarized in Figure 5. Most VOC species exhibited an 'U' shape trend during the whole observation, except for several VOCs (such as formaldehyde (HCHO) and methanol), which showed an increasing pattern. It should be noted that the measurement of HCHO could be strongly influenced by humidity. Since within the drift tube, the back reaction, which converse the protonated HCHO back into HCHO,

https://doi.org/10.5194/acp-2021-834
Preprint. Discussion started: 6 October 2021


Atmospheric Chemistry and Physics Discussions

is highly humidity dependent (Inomata et al., 2008; Warneke et al., 2011). To quantitatively evaluate the changes of individual VOC concentrations from Pre-lockdown to Full-lockdown period, when the variations of each VOCs are obvious, we applied MK trend test and Sen's slope analysis based on the hourly average VOCs concentration data.

Table 3 lists the top 10 VOCs species with decreasing pattern from Pre-lockdown to Full-lockdown period. Interestingly, toluene, benzene and xylene exhibited the most significant decreasing pattern, with a slope of 7.73×10^{-4}, 7.36×10^{-4}, and 7.20×10^{-4} ppbv h^{-1}, respectively. As for NO_x and TVOC, the slope was -1.62×10^{-2} and $5.48\ 10^{-3}$ ppb h^{-1}. This result corresponds with the drastic drop of industrial activities and traffic volumes, which are key sources of aromatics and NO_x, from Pre-lockdown to Full-lockdown period. Other VOCs, such as ethyl-acetate, acetic acid, acetaldehyde, diethyl sulfide, ethanol, butanol and acrolein are also tightly associated with industrial processes, thereby showed decreasing trend from Pre-lockdown to Full-lockdown period. Additionally, the average diurnal variations of acetonitrile, dimethyl formamide (DMF), and styrene, which are tracers of biomass burning and industrial emission, respectively, exhibited significant reduction during Full-lockdown period (Figure S1), also indicating strong decrease in these emissions. However, formaldehyde and methanol exhibited increasing trend, with a slope of 12.78×10^{-4} and 6.35×10^{-4} ppbv h^{-1}, respectively. This could be explained by the secondary formation of HCHO and methanol, which was promoted under better oxidation condition in Full-lockdown period.

https://doi.org/10.5194/acp-2021-834
Preprint. Discussion started: 6 October 2021

Atmospheric Chemistry and Physics Discussions

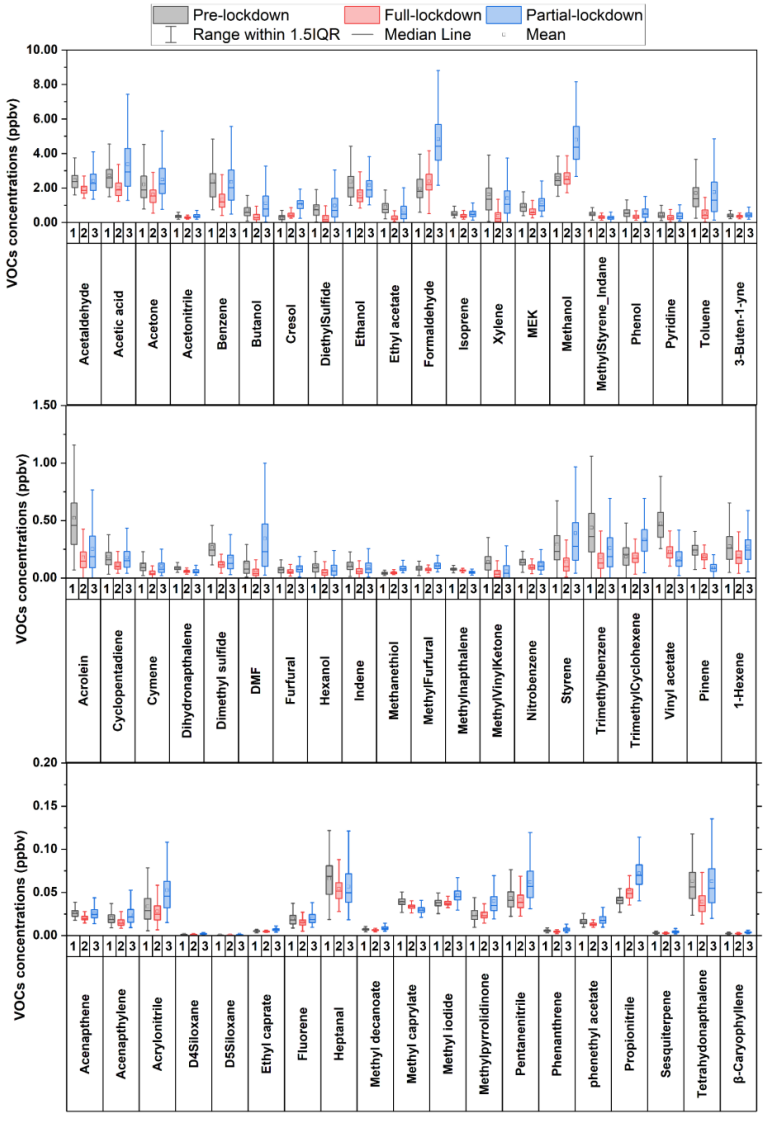

Figure 5. Concentrations of individual VOC species during different period.

***MEK, DMF, are abbreviation of Methyl ethyl ketone and dimethylformamide, respectively.**

https://doi.org/10.5194/acp-2021-834
Preprint. Discussion started: 6 October 2021

Atmospheric Chemistry and Physics Discussions

255 **Table 3. Top 10 VOCs with decreasing trend from Pre-lockdown to Full-lockdown**

VOC	Z value	Q *10000 (ppbv h^{-1})	VOC	Z value	Q *10000 (ppbv h^{-1})
Toluene	-14.02	-7.73	Acetaldehyde	-10.31	-3.95
Benzene	-9.65	-7.36	Diethyl sulfide	-9.15	-3.16
xylene	-12.38	-7.20	Ethanol	-5.48	-3.09
Ethyl-acetate	-18.53	-5.20	Butanol	-10.42	-2.83
Acetic acid	-6.79	-4.12	Acrolein	-15.48	-2.76

256 **3.2.3 Chemistry perspective**

257 The reactivities of different VOCs varies significantly, hence, ozone formation potential (OFP) is
258 used in this study to assess the potential contribution of active VOCs (including alkenes, aromatics and
259 OVCOs) to O_3 formation on the same basis, and it can be calculated by formula (5):

$$OFP_i = MIR_i \times [VOC_i] \quad (5)$$

260 where MIR_i is the ozone formation potential coefficient for a given VOC specie i in the maximum
261 increment reaction of O_3, acquired from Carter (2009); $[VOC_i]$ is the concentration of VOC species i (in
262 μg/m^3). The time series of total OFP is shown in Figure 6. The average OFP in Pre-lockdown, Full-
263 lockdown, and Partial-lockdown period was 269.4 ± 146.0, 147.2 ± 72.4, 279.3 ± 168.6 μg/m^3,
264 respectively. The trend of the total OFP indicates the drastic decrease of VOCs reactivities from Pre-
265 lockdown to Full-lockdown period. During Pre-lockdown period, aromatics were the dominant OFP
266 contributor (49%), followed by OVOCs (38%) and alkenes (13%) (Figure 4). Among aromatics, xylene
267 exhibited the maximum OFP value (68.6 ± 59.3 μg/m^3), followed by acetaldehyde (28.8 ± 6.4 μg/m^3),
268 toluene (25.7 ± 20.1 μg/m^3) trimethylbenzene (25.4 ± 15.8 μg/m^3), and formaldehyde (22.7 ± 9.1 μg/m^3)
269 (Figure S2), suggesting that anthropogenic emissions could be the main source of secondary formation
270 of O_3 during Pre-lockdown period. Compared to Pre-lockdown period, the OFP of aromatics decreased
271 dramatically (-91.2 μg/m^3) during Full-lockdown period (Figure 4 (B)), which was mainly attributed to
272 the rapid decline of human activities (e.g., transportation and industry). However, the OFP of alkenes
273 and OVOCs only decreased by 8.9 and 22.5 μg/m^3, respectively. As for alkene, this could be explained
274 by their chemical reactivities, which led to the fast degradation after emission. As for OVOCs, the
275 secondary formation could compensate the decrease in primary emissions. The OFP values of aromatics

https://doi.org/10.5194/acp-2021-834
Preprint. Discussion started: 6 October 2021

Atmospheric Chemistry and Physics Discussions

and alkenes during Pre-lockdown and Partial-lockdown period are comparable, but OVOCs exhibited higher OFP contribution (~46%) in Partial-lockdown period, which could be attributed to the higher AOC condition during Partial-lockdown period. To compare the average reactivity of VOCs during different periods, we calculate the mean MIR in each period. As shown in Figure 7, the average MIR during Pre-lockdown, Full-lockdown, and Partial-lockdown period was 3.85, 3.53 and 3.68 (g O_3/g VOC), respectively. This result suggests that the VOCs in Partial-lockdown should produce less O_3 than that in Pre-lockdown, and Partial-lockdown period. This is inconsistent with the observation, which shows relatively higher O_3 concentration during Full-lockdown period. However, the formation of O_3 was sensitive to the ratio of NO_x/VOCs and meteorological conditions, which can be significantly different in each period. As shown in Figure 7, the average NO_x/VOCs ratio in the three periods (shown in) was 1.84, 0.79, and 0.84, respectively, suggesting more NO_x was eliminated during Full-lockdown period, which could further influence the sensitivity of O_3 formation.

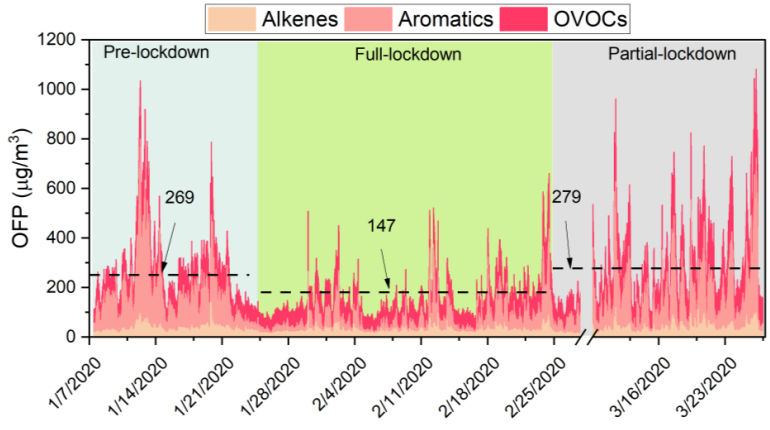

Figure 6. Time series of OFP during the whole observation period (dash lines represent the average OFP value during each period)

https://doi.org/10.5194/acp-2021-834
Preprint. Discussion started: 6 October 2021

Atmospheric Chemistry and Physics Discussions

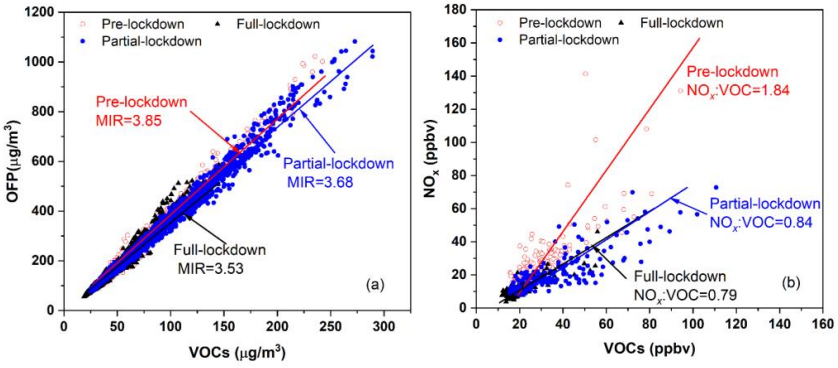

Figure 7. Plot of average MIR and NO_x vs VOCs during three periods.

To investigate the detailed formation mechanism of O_3 in each period, three cases (January 19th, February 1st, March 14th) with stagnant meteorological conditions were chosen. The index of agreement (IOA) of O_3 is 0.80, indicating that the model can capture the daytime variation of O_3. The simulated daytime OH concentrations exhibited an increasing trend from January 19 to March 14, with an average value of 0.36 ± 0.27 × 10^6, 0.75 ± 0.54 × 10^6 and 1.18 ± 0.78 × 10^6 molecules cm^{-3}, respectively. This could be attributed to the increasing solar radiation and temperature from January to March. To analyze the atmospheric oxidation, we calculated the AOC according to Eq(1). The average daytime AOC on Jan 19th, Feb 1st, and Mar 14th was 0.26 ± 0.35, 0.23 ± 0.33, and 0.31 ± 0.38 molecules cm^{-3} s^{-1}, respectively (Figure 9). Comparatively, these values are much lower than those simulated for Shanghai and Beijing (Liu et al., 2012; Zhu et al., 2020; Zhang et al., 2021) in summer, mainly due to the meteorological conditions in winter season. It is notable that the simulated OH on Jan 19th was significantly lower than that on Feb 14th, but the AOC on Jan 19th was comparable to that on Feb 1st. This should be ascribed to the abundant primary pollutants, which efficiently react with OH, during Pre-lockdown period.

https://doi.org/10.5194/acp-2021-834
Preprint. Discussion started: 6 October 2021

Atmospheric Chemistry and Physics Discussions

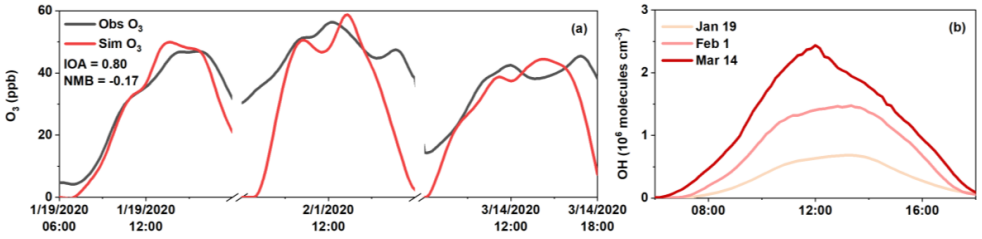

Figure 8. Comparison of simulated and observed O_3 (a) and simulated daytime OH concentrations (b) in three cases.

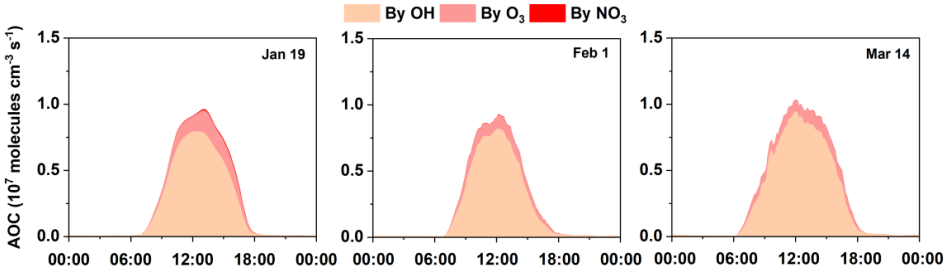

Figure 9. Diurnal variation of AOC in three cases

The daytime variations of OH reactivity calculated by OBM model are exhibited in Figure 10, including the contribution from measured pollutants (e.g., VOCs, NO*x*, and CO) and model-simulated species (OVOCs). Generally, the k_{OH} assessed at Changzhou was in the range of 9~32 s^{-1}, which was comparable to that calculated for other cities in China (e.g., Shanghai (4.6~25 s^{-1}, (Zhu et al., 2020)), Chongqing (15~25 s^{-1}, (Tan et al., 2019)) and Beijing (15~25 s^{-1}, (Tan et al., 2019))). It is obvious that OH reactivity peaked in the morning, with maximum values of 31.76, 17.98, and 17.30 s^{-1}, respectively. The OH reactivity from NO_2 exhibited obvious daytime variation, especially during the morning rush hour, which lead to the peak k_{OH} value during morning. The OH reactivity (k_{OH}) on Feb 1st was much lower than that in the other two cases, which was mainly due to the abundance of emissions during Pre-lockdown and Partial-lockdown period. Compared to Jan 19th, the k_{OH} from NO_2 on Feb 1st and Mar 14th showed lower levels, with an average value of 2.62 and 3.35 s^{-1}, respectively. This corresponds with the dramatic drop of traffic volume during lockdown periods. Similarly, compared to Jan 19, the k_{OH} from alkenes and aromatics were lower on Feb 1st and Mar 14th. It is notable that the OH reactivity from

https://doi.org/10.5194/acp-2021-834
Preprint. Discussion started: 6 October 2021

Atmospheric Chemistry and Physics Discussions

326 OVOCs kept almost stable in the three cases, this was mainly attributed to the stable OVOC
327 concentrations during these cases.

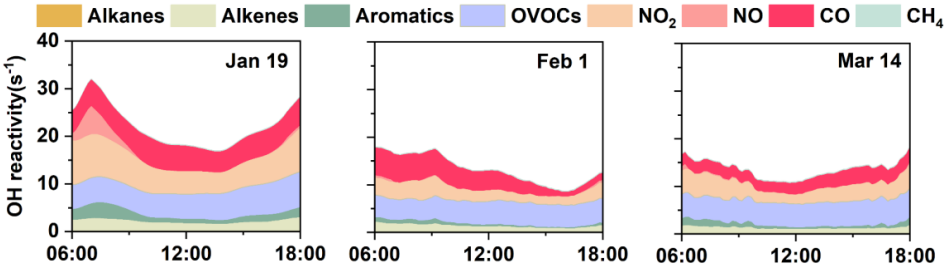

328

329 **Figure 10. Daytime variation of OH reactivity in three cases**

330 To investigate the variation of O_3 during different periods, the formation and loss pathways of O_3
331 were calculated (Figure 11). The formation of O_3 ($P(O_3)$) was dominated by HO_2+NO and RO_2+NO
332 pathways. Although the average MIR during Full-lockdown period was the minimum among the three
333 periods, the $P(O_3)$ on Feb 1st was higher than that on Jan 19th. This could be attributed to the higher
334 AOC and better photochemical conditions during Full-lockdown period. Similarly, much higher $P(O_3)$
335 was found on March 14th. To avoid the influence of meteorological conditions and test the potential
336 mean O_3 (MeanO_3) concentrations under different NO_x/VOCs ratios, a series of scenario analyses were
337 performed based on the average condition during the whole observation, and the isopleths of MeanO_3
338 concentrations are exhibited in Figure. 12. Note that the value of temperature and photolysis frequencies
339 (J values) in the scenario analyses could be higher than the actual value during Pre-lockdown period
340 and could further lead to overestimation of simulated MeanO_3 during Per-lockdown period. Additionally,
341 the VOCs concentrations mentioned in this section only represent the VOC species in the MCM
342 mechanism. By connecting the inflection points in each O_3 isopleth, we get the ridge line, which divides
343 the whole regime into NO_x-sensitive and VOCs-sensitive regimes (Figure. 12). During Pre-lockdown
344 period, the O_3 formation was in VOC-limited regime (triangles in Figure. 12), with an average
345 NO_x/VOC ratio of 1.84. As for Full-lockdown period, significant decrease of NO_x and VOC emissions
346 was observed, and the NO_x/VOCs ratio dropped to 0.79, which gradually switched the O_3 formation to
347 the junction of VOCs-limited and NO_x-limited regimes, especially on Feb 16th and Feb 17th (circles in
348 the red rectangle in Figure. 12), when the O_3 formation went into NO_x-limited regime. During Partial-

https://doi.org/10.5194/acp-2021-834
Preprint. Discussion started: 6 October 2021

Atmospheric Chemistry and Physics Discussions

lockdown period, increasing of VOCs and NO_x emission again dragged the formation of O_3 back into VOCs-limited regime (triangles in Figure. 12). Interestingly, although a great deal of NO_x and VOCs emissions were diminished during Full-lockdown period, the average MeanO_3 in Full-lockdown was supposed to be 2.4 ppbv higher than that in Pre-lockdown period. This result is consistent with the trend of the observed MDA8 O_3 and the results of the deweathered calculation. Therefore, the improper NO_x/VOCs reduction ratio and further influence on chemistry was the key reason for the abnormal increase of O_3 during Full-lockdown period in Changzhou in 2020.

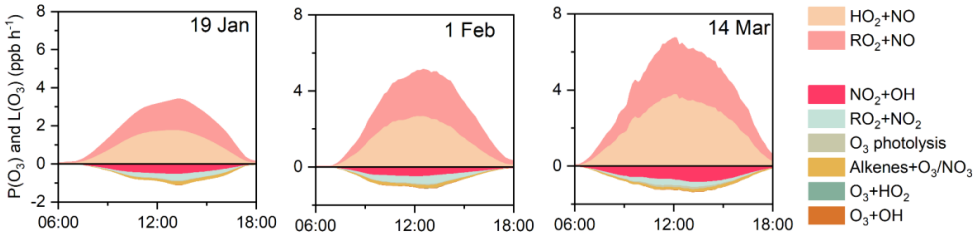

Figure 11. Daytime variation of P(O_3) and L(O_3) in three cases

https://doi.org/10.5194/acp-2021-834
Preprint. Discussion started: 6 October 2021

Atmospheric Chemistry and Physics Discussions

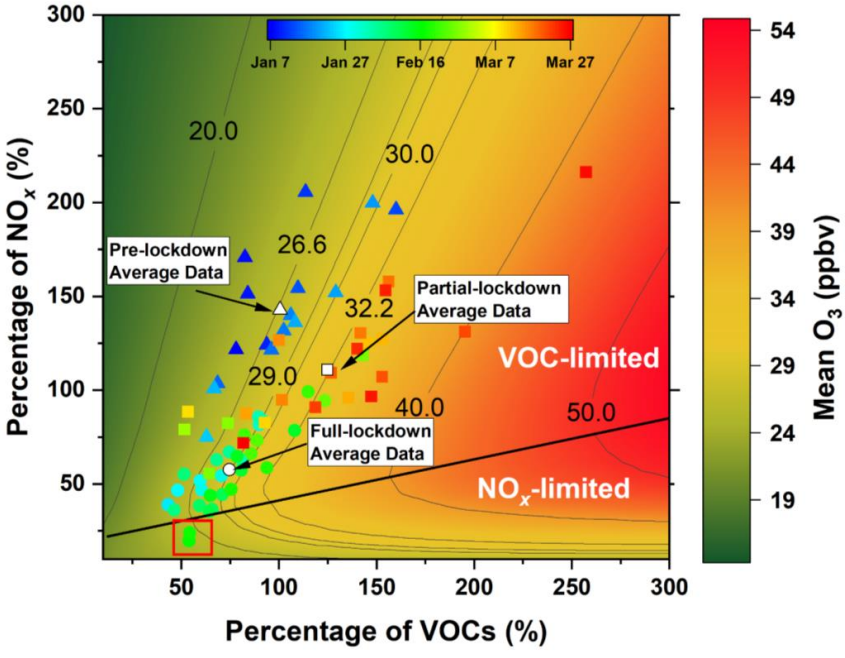

360

361 **Figure. 12 MeanO_3 isopleth. The colored circles, triangles, and rectangles represent the daily average**
362 **concentrations of NO_x and VOCs during Pre lockdown, Full-lockdown, and Partial-lockdown period,**
363 **respectively. The white circle, triangle, and rectangle indicates the average NO_x and VOCs concentrations**
364 **during Pre lockdown, Full-lockdown, and Partial-lockdown period, respectively.**

365 The scenario analyses raise a question: how much O_3 would change as a function of reduction of
366 NO_x and VOCs? Therefore, the reduction percentage of O_3 ($\Delta O_3/O_3$) during Pre-lockdown period as a
367 function of reduction of VOCs and NO_x were calculated, and the result could be regarded as a potential
368 to control O_3 pollution. Based on the VOCs species in MCM v3.3.1, we classified the measured VOCs
369 into four groups: alkenes (n-butene); aromatics (including benzene, toluene, phenol, xylene, styrene,
370 cresol, and trimethylbenzene); OVOCs (including methanol, ethanol, formaldehyde, aldehyde, acrolein,
371 methyl vinyl ketone, methyl ethyl ketone, ethyl acetate, methyl isobutyl ketone, hexanol, and heptanal);
372 and BVOCs (isoprene, pinene, and caryophyllene). The results in Figure 13(a) indicate that more
373 reduction potential of O_3 could be achieved by diminishing aromatics, followed by BVOCs, OVOCs,
374 and alkenes. It should be noted that many light alkanes and active alkenes, such as ethene and propene,

https://doi.org/10.5194/acp-2021-834
Preprint. Discussion started: 6 October 2021

Atmospheric Chemistry and Physics Discussions

could not be measured by the PTR-TOF-MS and might further lead to the underestimation of ozone sensitivity to alkanes and alkenes. Additionally, this comparison has a drawback of being influenced by the concentrations of VOCs. To normalize the influence of concentrations of VOCs, the descent rate of O_3 (ΔO_3 (ppbv)/ ΔVOCs (ppbv)) as a function of reduction percentage of VOCs were calculated (Figure 13 (b)). O_3 exhibited the highest dependence on BVOCs, with an average descent rate of 3.74 ± 0.09 ppbv/ppbv. Differing from the result in Figure 13 (a), diminishing alkenes could lead to decreasing of O_3 by an average descent rate of 1.69 ± 0.01 ppbv/ppbv. On the contrary, reduction of NO_x would lead to increase of O_3, with an average rate of 1.29 ± 0.21 ppbv/ppbv (Figure S3). Although the descent rate of O_3 turned to decrease and the sensitive of O_3 formation get into NO_x-limited regime when over 70% of NO_x were eliminated, it still causes net increase of O_3.

Although diminishing BVOCs seems to the most efficient way to restrain O_3 pollution, most of BVOCs were emitted directly from plants and could not be easily controlled. Besides, huge number of OVOCs (such as formaldehyde, aldehyde, methanol, ethanol, methyl vinyl ketone, methyl ethyl ketone, etc.) could be directly emitted from anthropogenic processes or secondary formatted from the oxidation of precursors (such as alkenes and aromatics), which complicates the control of OVOCs. Therefore, considering the reduction potential and descent rate of O_3, more efforts are needed on the control of alkenes and aromatics.

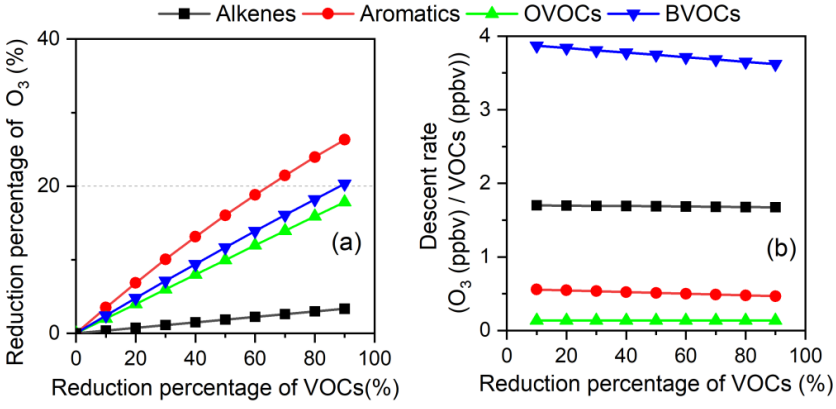

Figure 13. Reduction percentage of O_3 as a function of reduction percentage of VOCs (a); descent rate of O_3 as a function of reduction percentage of VOCs (b).

https://doi.org/10.5194/acp-2021-834
Preprint. Discussion started: 6 October 2021


Atmospheric Chemistry and Physics Discussions

4. Conclusions

After the outbreak of COVID-19, strict epidemic prevention measures have been adopted throughout China, leading to dramatic decrease in traffic volume and industrial activities. Affected by the decrease of number of vehicles on the road, non-essential industrial productivity, and associated pollutant emissions, most of the air pollutants (e.g., $PM_{2.5}$, PM_{10}, NO, NO_2, SO_2, and VOCs) dropped to a lower level during lockdown period (especially during Full-lockdown period). However, O_3 increased compared to that during the same period in 2019 in many urban areas of China. To figure out the reasons for this abnormal increase of O_3, the characteristics of O_3 precursors (NO_x, VOCs) during Pre-lockdown, Full-lockdown, and Partial-lockdown periods in Changzhou were analyzed. Although this study was conducted in single city of China, the representativeness of Changzhou guaranteed the applicability of the results the YRD region. Results suggested that the decrease of human activities during Full-lockdown period significantly suppressed the emissions of NO_x and VOCs, which further lead to dramatic drop in the concentrations of most VOCs, especially aromatics. As a result, the NO_x/VOCs ratios dropped from 1.84 at Pre-lockdown period to 0.79 during Full-lockdown period. By deweathered calculation, we found that meteorology only contributed a minor positive (0.5 ppbv) value to the increase of O_3, whereas changes in precursor emissions led to 5.1 ppbv increase in O_3 concentrations during Full-lockdown period. To verify this result, a box model was used to simulate the formation of O_3. Results show that the AOC level during Full-lockdown was comparable to that during Pre-lockdown period, but the formation rate of O_3 was much higher during Full-lockdown period. By scenario analysis, we found the decrease of NO_x and VOCs in Full-lockdown period dragged the formation of O_3 from VOC-sensitive regime to the junction of VOCs- and NO_x-limited regime, and the average simulated MeanO_3 in Full lockdown period could be 2.4 ppbv higher than that in Pre-lockdown period. Although the deweathered model and OBM model shows differences in the emission-derived change of O_3, the results together point out that the improper reduction of NO_x and VOCs was the key reason for the abnormal increase of O_3 during Full-lockdown period in 2020. Overall, the outbreak of COVID-19 has caused devastation over the world. However, it provided an extreme experiment to

https://doi.org/10.5194/acp-2021-834
Preprint. Discussion started: 6 October 2021


Atmospheric Chemistry and Physics Discussions

421 investigate the O_3 formation under strict emission control policies and provided insights into the policy
422 formulation for diminishing O_3 pollution in the YRD region. The data indicate that the concentrations
423 of VOCs and NO_x have changed dramatically during the pandemic, a common situation also found in
424 other Chinese cities, and led to the switch of O_3 formation sensitivity. These results have a clear
425 indication that, in the future, more efforts should be paid on the reduction ratio of anthropogenic VOCs
426 and NO_x.

427 ## Acknowledgement

428 This study was financially sponsored by the National Natural Science Foundation of China (grant
429 42075144, 41875161, 42005112), the Shanghai Science and Technology Innovation Plan (no.
430 19DZ1205007), the Shanghai Sail Program (no. 19YF1415600), the Shanghai International Science and
431 Technology Cooperation Fund (no. 19230742500).

432 ## References

433 Alhathloul SH, Khan AA, Mishra AK. Trend analysis and change point detection of annual and seasonal
434 horizontal visibility trends in Saudi Arabia. Theoretical and Applied Climatology 2021; 144: 127-
435 146.
436 Jensen A, Liu ZQ, Tan W, Dix B, Chen TS, Koss A, Zhu L, Li Li, Gouw J. Measurements of Volatile Organic
437 Compounds during the COVID-19 Lockdown in Changzhou, China. Geophysical Research Letters
438 2021. (*In production*)
439 Carter W. Updated maximum incremental reactivity scale and hydrocarbon bin reactivities for regulatory
440 applications. California Air Resources Board Contract 2009; 339.
441 Cheng Z, Zhang J, Zhou J, Sun J, Zhou W, Chen C, et al. Air pollutant emission inventory and distribution
442 characteristics in Changzhou (in Chinese). The Administration and Technique of Environmental
443 Monitoring 2016; 28: 24-28.
444 Fan L, Fu S, Wang X, Fu Q, Jia H, Xu H, et al. Spatiotemporal variations of ambient air pollutants and
445 meteorological influences over typical urban agglomerations in China during the COVID-19
446 lockdown. Journal of Environmental Sciences (China) 2021; 106: 26-38.
447 Fu X, Wang S, Zhao B, Xing J, Cheng Z, Liu H, et al. Emission inventory of primary pollutants and chemical

https://doi.org/10.5194/acp-2021-834
Preprint. Discussion started: 6 October 2021


Atmospheric Chemistry and Physics Discussions

448 speciation in 2010 for the Yangtze River Delta region, China. Atmospheric Environment 2013; 70:
449 39-50.
450 Gao C, Li S, Liu M, Zhang F, Achal V, Tu Y, et al. Impact of the COVID-19 pandemic on air pollution in
451 Chinese megacities from the perspective of traffic volume and meteorological factors. Science of
452 The Total Environment 2021; 773: 145545.
453 Huang L, Liu Z, Li H, Wang Y, Li Y, Zhu Y, et al. The Silver Lining of COVID-19: Estimation of short-term
454 health impacts due to lockdown in the Yangtze River Delta Region, China. GeoHealth 2020; 4:
455 e2020GH000272.
456 Inomata, S., Tanimoto, H., Kameyama, S., Tsunogai, U., Irie, H., Kanaya, Y., Wang, Z. J. A. C., and Physics:
457 Determination of formaldehyde mixing ratios in air with PTR-MS: laboratory experiments and field
458 measurements, 8, 273-284, 2008.
459 Li, L., An, J., Huang, L., Yan, R., Huang, C., and Yarwood, G. Ozone source apportionment over the Yangtze
460 River Delta region, China: Investigation of regional transport, sectoral contributions and seasonal
461 differences, Atmospheric Environmental 2019; 202, 269–280.
462 Li L, Li Q, Huang L, Wang Q, Zhu A, Xu J, et al. Air quality changes during the COVID-19 lockdown over
463 the Yangtze River Delta Region: An insight into the impact of human activity pattern changes on air
464 pollution variation. Science of the Total Environment 2020; 732:139282.
465 Liu Z, Wang Y, Gu D, Zhao C, Huey LG, Stickel R, et al. Summertime photochemistry during CAREBeijing-
466 2007: RO_x budgets and O_3 formation. Atmospheric Chemistry and Physics 2012; 12: 7737-7752.
467 Maji S, Beig G, Yadav R. Winter VOCs and OVOCs measured with PTR-MS at an urban site of India: Role
468 of emissions, meteorology and photochemical sources. Environmental Pollution 2020; 258: 113651.
469 Pathakoti M, Santhoshi T, Aarathi M, Mahalakshmi DV, Kanchana AL, Srinivasulu J, et al. Assessment of
470 Spatio-temporal Climatological trends of ozone over the Indian region using Machine Learning.
471 Spatial Statistics 2021; 43: 100513.
472 Sen PK. Estimates of the regression coefficient based on Kendall's tau. Journal of the American statistical
473 association 1968; 63: 1379-1389.
474 Shen L, Zhao T, Wang H, Liu J, Bai Y, Kong S, et al. Importance of meteorology in air pollution events
475 during the city lockdown for COVID-19 in Hubei Province, Central China. Science of the Total

https://doi.org/10.5194/acp-2021-834
Preprint. Discussion started: 6 October 2021


Atmospheric Chemistry and Physics Discussions

476 Environment 2021; 754, 142227.
477 Shi, X., Ge, Y., Zheng, J., Ma, Y., Ren, X., and Zhang, Y. Budget of nitrous acid and its impacts on
478 atmospheric oxidative capacity at an urban site in the central Yangtze River Delta region of China,
479 Atmospheric Environment 2020; 238.
480 Sun K, Zhou J, Ding H, Chen X, Liu Z, Xue P. Anthropogenic source VOCs emission inventory of Changzhou
481 city (in Chinese). Environmental Monitoring and Forewarning 2019; 11: 57-62.
482 Tan ZF, Lu KD, Jiang MQ, Su R, Wang HL, Lou SR, et al. Daytime atmospheric oxidation capacity in four
483 Chinese megacities during the photochemically polluted season: a case study based on box model
484 simulation. Atmospheric Chemistry and Physics 2019; 19: 3493-3513.
485 Valach AC, Langford B, Nemitz E, Mackenzie AR, Hewitt CN. Seasonal and diurnal trends in concentrations
486 and fluxes of volatile organic compounds in central London. Atmospheric Chemistry and Physics
487 2015; 15: 7777-7796.
488 Venter ZS, Aunan K, Chowdhury S, Lelieveld J. COVID-19 lockdowns cause global air pollution declines.
489 Proceedings of the National Academy of Sciences of the United States of America 2020; 117: 18984-
490 18990.
491 Warneke, C., Veres, P., Holloway, J., Stutz, J., Tsai, C., Alvarez, S., Rappenglueck, B., Fehsenfeld, F., Graus,
492 M., and Gilman, J. J. A. M. T.: Airborne formaldehyde measurements using PTR-MS: calibration,
493 humidity dependence, inter-comparison and initial results, 4, 2345-2358, 2011.
494 Wolfe GM, Marvin MR, Roberts SJ, Travis KR, Liao J. The Framework for 0-D Atmospheric Modeling
495 (F0AM) v3.1. Geoscientific Model Development 2016; 9: 3309-3319.
496 Xu L, Zhang J, Sun X, Xu S, Shan M, Yuan Q, et al. Variation in concentration and sources of black carbon
497 in a megacity of China during the COVID-19 pandemic. Geophysical Research Letters 2020; 47:
498 e2020GL090444.
499 Zhang D, Cong Z, Ni G. Comparison of three Mann-Kendall methods based on the China's meteorological
500 data. Shuikexue Jinzhan/Advances in Water Science 2013; 24: 490-496.
501 Zhang, K., Huang, L., Li, Q., Huo, J., Duan, Y., Wang, Y., Yaluk, E., Wang, Y., Fu, Q., and Li, L.: Explicit
502 modeling of isoprene chemical processing in polluted air masses in suburban areas of the Yangtze
503 River Delta region: radical cycling and formation of ozone and formaldehyde, Atmos. Chem. Phys.,

https://doi.org/10.5194/acp-2021-834
Preprint. Discussion started: 6 October 2021

Atmospheric Chemistry and Physics Discussions

21, 5905-5917, 10.5194/acp-21-5905-2021, 2021.

Zhang K, Li L, Huang L, Wang Y, Huo J, Duan Y, et al. The impact of volatile organic compounds on ozone formation in the suburban area of Shanghai. Atmospheric Environment 2020a; 232: 117511.

Zhang K, Xu J, Huang Q, Zhou L, Fu Q, Duan Y, et al. Precursors and potential sources of ground-level ozone in suburban Shanghai. Frontiers of Environmental Science and Engineering 2020b; 14: 1-12.

Zheng H, Kong S, Chen N, Yan Y, Liu D, Zhu B, et al. Significant changes in the chemical compositions and sources of $PM_{2.5}$ Wuhan since the city lockdown as COVID-19. Science of the Total Environment 2020; 739: 140000.

Zhu J, Wang S, Wang H, Jing S, Lou S, Saiz-Lopez A, et al. Observationally constrained modeling of atmospheric oxidation capacity and photochemical reactivity in Shanghai, China. Atmospheric Chemistry and Physics 2020; 20: 1217-1232.